Climate Dynamics (2019) 53:5909–5925
https://doi.org/10.1007/s00382-019-04904-z

Regional modeling of surface mass balance on the Cook Ice Cap, Kerguelen Islands (49°S, 69°E)

Deborah Verfaillie[1] · Vincent Favier[2] · Hubert Gallée[2] · Xavier Fettweis[3] · Cécile Agosta[3,4] · Vincent Jomelli[5]

Received: 14 June 2018 / Accepted: 17 July 2019 / Published online: 3 August 2019

Abstract
We assess the ability of the regional circulation model MAR to represent the recent negative surface mass balance (SMB) observed over the Kerguelen Islands (49°S, 69°E) and evaluate the uncertainties in SMB projections until the end of the century. The MAR model forced by ERA-Interim reanalysis shows a good agreement with meteorological observations at Kerguelen, particularly after slight adjustment of the forcing fields (+ 10% humidity, + 0.8 °C, all year round) to improve precipitation occurrence and intensity. The modeled SMB and surface energy balance (SEB) are also successfully evaluated with observations, and spatial distributions are explained as being largely driven by the elevation gradient and by the strong west to east foehn effect occurring on the ice cap. We select five general circulation models (GCMs) from the Coupled Model Intercomparison Project phase 5 (CMIP5) by evaluating their ability to represent temperature and humidity in the southern mid-latitudes over 1980–1999 with respect to ERA-Interim and use them to force the MAR model. These simulations fail to replicate SMB observations even when outputs from the best CMIP5 model (ACCESS1-3) are used as forcing because all GCMs fail in accurately reproducing the circulation changes observed at Kerguelen since the mid-1970s. Global models chosen to represent extreme values of SMB drivers also fail in producing extreme values of SMB, suggesting that more rigorous modeling of present and future circulation changes with GCMs is still needed to accurately assess future changes of the cryosphere in this area.

Keywords Surface mass balance · Regional climate model · Subantarctic · Reanalyses · CMIP5

1 Introduction

Regions located between 45 and 55°S constitute the meeting point between tropical and polar air masses, resulting in some intense cyclonic activity influencing the global atmospheric circulation (Garreaud et al. 2009; Thompson et al. 2011; Purich et al. 2013). Low temperature and high humidity advected by the westerly winds (inside so-called storm tracks) enabled the formation of ice caps at low elevations in these sub-polar regions (Fitzharris et al. 1997; Takeuchi et al. 1999; Fitzharris et al. 2007; Garreaud et al. 2009). Among those, the Cook Ice Cap on the Kerguelen Islands (49°S, 69°E) in the Southern Indian Ocean has experienced one of the largest wastages (melting or evaporation of ice/snow) over the last 15 years (Verfaillie et al. 2015; Favier et al. 2016). However, the future evolution of the Cook Ice Cap remains unclear because its wastage was largely controlled by the recent southern hemisphere storm track shift, and future precipitation changes remain highly uncertain in GCM projections.

Electronic supplementary material The online version of this article (https://doi.org/10.1007/s00382-019-04904-z) contains supplementary material, which is available to authorized users.

✉ Deborah Verfaillie
deborah.verfaillie@gmail.com

[1] Barcelona Supercomputing Center, Barcelona, Spain

[2] Institut des Géosciences de l'Environnement UGA/CNRS/IRD/G-INP, CS 40 700, 38058 Grenoble Cedex 9, France

[3] Department of Geography, University of Liège, Liège, Belgium

[4] Laboratoire des Sciences du Climat et de l'Environnement, LSCE/IPSL, CEA-CNRS-UVSQ, Université Paris-Saclay, 91198 Gif-sur-Yvette, France

[5] Université Paris 1 Pantheon-Sorbonne, CNRS Laboratoire de Géographie Physique, 92195 Meudon, France

The processes involved in glacial mass balance occur at small spatial scales (typically a meter to a few kilometers), and thus downscaling must be carried out, usually by using Atmosphere-Ocean General Circulation Models (AOGCMs, resolution of several tens or hundreds of kilometers) to drive regional climate models (RCMs, resolution of a few kilometers). The ability of RCMs to accurately model glaciers and ice cap SMB has frequently been tested (Fettweis et al. 2013; Schaefer et al. 2013) and represents the first step to assess glacier SMB projections. Such a dynamical downscaling step is also necessary for future SMB projections even though the accuracy of modeling first depends on AOGCM ability to accurately simulate the regional climate. Indeed, numerous previous studies have used outputs from CMIP3 or CMIP5 (Coupled Model Intercomparison Project phase 3 and 5, Taylor et al. 2012) GCMs as such (Falvey and Garreaud 2009; Thompson et al. 2011; Purich et al. 2013; Wang and Kay 2013), to drive RCMs (Schaefer et al. 2013; Cabré et al. 2016) or other climate or impact models (Marzeion et al. 2012; Delworth and Zeng 2014; Radić et al. 2014) in the southern sub-polar latitudes. However, Favier et al. (2016) showed that most CMIP5 GCMs are unable to correctly reproduce glacier wastage in regions characterized by strong precipitation decrease, like the Kerguelen Archipelago (southern Indian Ocean), and that outputs from these models should first be corrected (at least for mean temperature and precipitation biases compared to observations) before using them to force RCMs or other models. Moreover, producing multi-decadal simulations of climate using an ensemble of RCMs requires much computing time, and using a multi-model mean would not prove useful because of its inaccurate positioning of the storm tracks and representation of their shift (Favier et al. 2016). Several studies have shown this discrepancy of CMIP5 GCMs and proposed to select only few models that correctly represent the local climate settings (Fettweis et al. 2013; Agosta et al. 2015). Here we select a few CMIP5 GCMs based on their accurate representation of the 1980–1999 climate (temperature and humidity in the free troposphere) in the southern Indian Ocean, evaluated against ERA-Interim, the best available reanalysis data in this region. These GCMs are then used to force an RCM centered on the Kerguelen Islands, and we analyze the surface mass balance results for the recent period (1980–2005) and the 21st century.

In the present study we investigate the recent glacial retreat of the main ice body on the Kerguelen Islands, the Cook Ice Cap, a region marked by fast-changing climate linked to circulation changes promoting a precipitation decrease (Favier et al. 2016). We determine whether this glacial retreat can be modeled using the MAR (Modèle Atmosphérique Régional, Gallée and Schayes 1994) regional model forced by ERA-Interim and by selected CMIP5 AOGCMs. After presenting the materials and methods (Sect. 2), atmospheric outputs of the MAR driven by the ERA-Interim reanalysis are evaluated against observations and their spatial representation is analyzed (Sect. 3.1). Surface mass balance and surface energy balance (SEB) obtained from MAR, forced by outputs from ERA-Interim are assessed in Sect. 3.2. Subsequently, results concerning the selection of CMIP5 GCMs are presented (Sect. 3.3). Finally, surface mass balance (SMB) over the last decades and future projections modeled using the MAR driven by these selected models are critically examined (Sect. 3.4) and discussed (Sect. 4).

2 Materials and methods

2.1 Study site

The Kerguelen Islands (49°S, 69°E) are located in the southern Indian Ocean (Fig. 1) and form a unique sub-polar observation site due to the scarcity of glacier-covered zones in this area (Verfaillie et al. 2015; Favier et al. 2016). Their glaciers, located on low-lying islands, are directly influenced by the ocean and the associated atmospheric variations (Poggi 1977a, b; Vallon 1987; Jomelli et al. 2017, 2018). Following relative stability between the 1800s and the 1960s (Frenot et al. 1993), the Cook Ice Cap retreated extremely rapidly, losing 20% of its surface area in 40 years (Berthier et al. 2009). This acceleration has initially been attributed to warming (Frenot et al. 1993, 1997; Berthier et al. 2009) but was recently proven to be associated to a reduction of precipitation on the archipelago due to circulation changes induced by the strengthening of the Southern Annular Mode (Verfaillie et al. 2015; Favier et al. 2016).

2.2 The regional climate model MAR

2.2.1 Model description

The model used in this study is the regional climate model MAR (version 3.3, Fettweis et al. 2017), coupled to the 1D surface scheme SISVAT (Soil Ice Snow Vegetation Atmosphere Transfer) through the exchange of energy fluxes. This limited area model fully resolves the continuity equation (Gallée and Schayes 1994). It is a hydrostatic model solving primitive equations, and uses sigma pressure coordinates. The mass conservation equation is written in its compressible form, i.e. without approximation. A cloud microphysics model is also included, solving the conservation equations of the concentration of cloud droplets, water drops, cloud ice crystals and snow crystals based on Kessler (1969) and Lin et al. (1983). Bechtold et al. (2001)'s convective scheme is used. Radiative schemes implemented are based on Fouquart and Bonnel (1980) for solar radiation and Morcrette (2002)

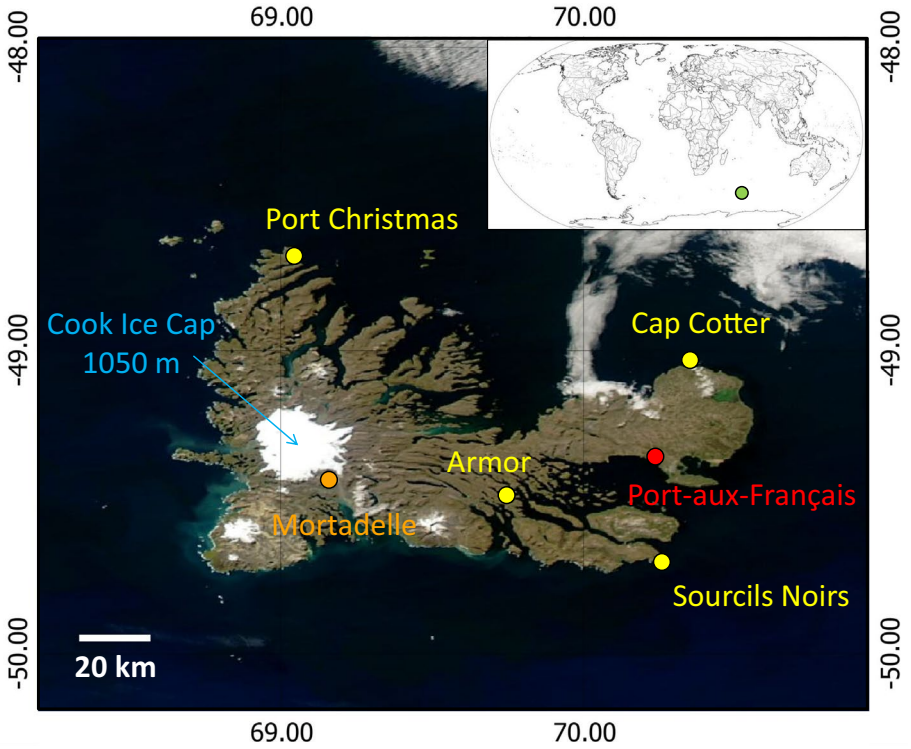

Fig. 1 MODIS© image of the Kerguelen Islands showing the Cook Ice Cap and the location of Port-aux-Français scientific station where the Météo France meteorological station is installed. The five other meteorological stations used in this study are also indicated (in yellow and orange). The location of the Kerguelen Islands is indicated by the green dot on the world map in the top right corner. Adapted from Verfaillie et al. (2015)

for the infrared. The constitutive equations of the MAR model are presented in detail in Gallée and Schayes (1994).

To compute glacier surface mass balance an energy balance approach is used through SISVAT. The SISVAT surface scheme (De Ridder and Gallée 1998; Gallée et al. 2001) determines the exchanges between the different surface components. SISVAT includes a vegetation and soil unit as well as a snow and ice unit. In the case of Kerguelen, devoid of trees, the only vegetation considered is tundra. Pixels can thus be partly covered by snow or ice, bare soil, tundra or water (ocean or lakes). The unit describing snow and ice in SISVAT was developed by Gallée and Duynkerke (1997), Gallée et al. (2001) and Lefebre et al. (2002). It is a multi-layer model that determines the exchanges between the surface of the ice cap, sea ice (not present in the Kerguelen Islands), snow-covered tundra and the atmosphere. The soil and vegetation unit was developed by De Ridder and Gallée (1998). SISVAT accounts for water percolation and refreezing in the snowpack, pore closure in the firn and meltwater runoff on ice and its influence on the albedo. Heat conduction in the snow is based on Yen (1981). The snow metamorphism parameterization is based on the CROCUS model (Brun et al. 1992), which enables a fine representation of surface albedo depending on the size and shape of snow grains. Turbulent fluxes are calculated following Monin and Obukhov (1954) similarity theory, by using the relationships between fluxes and gradients from Duynkerke and van den Broeke (1994). This scheme has been validated for cold glaciers in Antarctica (Gallée and Schayes 1994; Gallée et al. 2001), over melting zones in Greenland (Gallée and Duynkerke 1997), and also for other regions such as the Himalayas (Ménégoz et al. 2013).

2.2.2 Model inputs

The MAR RCM was forced at its lateral boundaries by 6-h meteorological fields (temperature, humidity, winds and pressure) from the ERA-Interim reanalysis dataset (Dee et al. 2011) or CMIP5 (Coupled Model Intercomparison Project phase 5) GCM output. Daily sea ice concentration and sea-surface temperature data from the reanalysis data and CMIP models were also prescribed into MAR as surface oceanic conditions. Topography in the MAR regional model was taken from the global topographic model ETOPO1 [1 arc-minute resolution, Amante and Eakins (2009)], which gives a better representation of the topography on the Kerguelen Islands than other topographic models such as ETOPO5 or GTOPO30. We used the ERA-Interim reanalysis data from the European Centre for Medium-Range Weather Forecasts (ECMWF), and outputs from 5 different CMIP5 GCMs selected from the CMIP5 ensemble after a critical analysis of the capabilities of the reanalysis data and the different models to reproduce the regional climate settings (Sect. 2.4). Models selected were: ACCESS1-3 (Commonwealth Scientific and Industrial Research Organisation, and Bureau of Meteorology, Australia), MRI-CGCM3 (Meteorological

Research Institute, Japan), GFDL-CM3 (National Oceanic and Atmospheric Administration Geophysical Fluid Dynamics Laboratory, USA), GISS-E2-R (National Aeronautics and Space Administration Goddard Institute for Space Studies, USA) and NorESM1-M (Norwegian Climate Centre, Norway).

Reanalysis datasets consist of output from a model using data assimilation, i.e. combining observations (from radiosondes, buoys, satellites, etc.) and prior forecast model information, to obtain a physically coherent estimate of the state of the atmosphere that is as close to reality as possible. Each reanalysis is produced with a single version of a data assimilation system. Surface and radiosonde observations performed at Port-aux-Français (PAF) have been assimilated in the reanalyses since 1979 for ERA-Interim (Dee et al. 2011). CMIP5 (Taylor et al. 2012) gathers 20 climate study groups, which produced long-term simulations (centennial scale) using atmosphere-ocean global climate models (AOGCMs) sometimes also coupled to a carbon cycle model, initialized from pre-industrial simulations. In this study, we used outputs from the historical (1950–2005) and future (2006–2100) RCP 8.5 CMIP5 scenarios (long-term experiments). A list of the different CMIP5 models analyzed here is given in Supplementary Table S1.

2.2.3 Simulations

The MAR model was run on a grid centered on the Kerguelen Islands, at a resolution of 10 km (800 × 800 km domain). In the configuration used for this study the model has 23 atmospheric sigma levels, from $\sigma = 0.11$ (an altitude of ~ 15 km) to $\sigma = 0.9998$ (3 m above the surface).

For SMB estimates, the 8 MAR grid cells partially or entirely covered by ice at the location of the Cook Ice Cap were used to derive the relation between SMB at individual grid cells and the cells' elevation. Hypsometry (i.e. the relation between glacier surface area and elevation) of the Cook Ice Cap in 2009 (Verfaillie et al. 2015) was then used for extrapolating the 1980–2005 MAR SMB to the whole ice cap. For SEB estimates, only the 5 MAR grid cells where the ice mask exceeded 75% were considered, in order to avoid biases in air temperature resulting from the warming of bare soil or tundra-covered adjacent surfaces.

2.3 Meteorological and glaciological network for evaluation

MAR outputs of daily precipitation and near-surface temperature were evaluated against observations from weather stations installed in six different locations on the Kerguelen Islands. Figure 1 shows the location of each station. Direct meteorological measurements have been routinely collected by Météo France at the station of Port-aux-Français (29 m a.s.l.) since 1950. The automatic weather station (AWS) of La Mortadelle was installed in December 2010 on a rock outcrop close to the Cook Ice Cap (see Verfaillie et al. (2015) for more details about Port-aux-Français and La Mortadelle stations). Additionally, four new meteorological stations (Port Christmas, Cap Cotter, Sourcils Noirs and Armor, see Fig. 1) were set up in 2012 in the framework of the LEFE-KCRUMBLE project, in order to gain insight into the spatial variability of climate on the archipelago. At Port Christmas, only temperature measurements are available because precipitation is biased by moisture transport from the lake located just upwind. Characteristics of the different sensors of the stations can be found in Table 1. Additionally, for SMB and SEB evaluation, the 2011 glaciological network presented in Verfaillie et al. (2015) was used, as well as stake measurements carried out in the 1970s (Vallon 1977a, b, 1987); these have previously been used and described in Verfaillie et al. (2015).

2.4 Selection of CMIP5 global models

As a first attempt to give a range of SMB estimates on the Cook Ice Cap for the recent period (1980–2005), we used a method derived from that developed by Fettweis et al. (2013) over Greenland to select the most suitable CMIP5 GCMs and to determine the two models that would yield the most extreme climate. This method was used and further refined (using 5 different fields for the GCM selection) over the whole Antarctic continent by Agosta et al. (2015). In this method, fields from the reanalysis closest to observations, i.e. generally the ERA-Interim reanalysis, are used to select the models, over the period 1980–1999 (used by Fettweis et al. (2013) and Solomon et al. (2007) as the reference period for the current climate). Surface and radiosonde observations performed at the station of Port-aux-Français on the Kerguelen Islands are assimilated daily in the ERA-Interim reanalysis. The latter was satisfactorily evaluated against in-situ observations of temperature, precipitation and shortwave and longwave radiation by Verfaillie et al. (2015).

To correctly represent the surface mass balance on the Kerguelen Islands, temperature and precipitation are the

Table 1 Characteristics of sensors installed on the LEFE-KCRUMBLE stations: name, data measured, accuracy (according to the manufacturer) and measurement height

Name	Data	Accuracy	Height (m)
Young anemometer 05103	Wind speed	± 0.3 m s^{-1}	2
	Wind direction	± 3°	
CS215	Air temperature	± 0.9 °C	2
	Relative humidity	± 4%	
CS ARG100 pluviometer	Precipitation	± 8%	1

most important parameters (Favier et al. 2016). Summer temperature controls ablation on the surface of the ice cap, which is temperate and thus very sensitive to small variations around 0°C. Moreover, the influence of the Southern Annular Mode on temperature is strong in summer. For each CMIP5 GCM and for ERA-40 (ECMWF, Uppala et al. 2005) and NCEP1 (National Centers for Environmental Prediction, National Center for Atmospheric Research NCEP-NCAR, Kalnay et al. 1996) reanalyses, a comparison with ERA-Interim is performed for the summer (December, January and February) mean temperature at 850 hPa, impacting the melt at the surface of the ice cap. Biases are calculated on the whole 40°–60°S latitudinal belt as: $(\overline{X}_{CMIP5} - \overline{X}_{ERA-Int})/\sigma(X_{ERA-Int})$, where X is the variable of interest and σ represents the standard deviation. Precipitation controls the accumulation on the ice cap and is driven by regional circulation and the position of the storm tracks. However, precipitation is not used as a forcing field in the MAR model, which simulates its own precipitation based on the forcing fields of temperature, wind, humidity and pressure. Thus specific humidity at 850 hPa was also analyzed against ERA-Interim. Similarly, Agosta et al. (2015) use the precipitable water field as a proxy of precipitation. Unlike Fettweis et al. (2013), wind speed was not taken into account, because variations in the wind field are not so important in the Kerguelen Islands due to the general westerly flow in this region. Anomalies of the 850 hPa summer temperature and the 850 hPa specific humidity with respect to ERA-Interim over 1980–1999 for all CMIP5 GCMs and ERA-40 and NCEP1 reanalyses are presented in Figs. S1 and S2 respectively.

3 Results

3.1 Evaluation of MAR atmospherical outputs against observations

MAR outputs were evaluated against observations from weather stations installed on six locations of the Kerguelen Islands (Sect. 2.3), for different time periods depending on the data available. Figure 2 and Table 2 give an overview of temperature and precipitation outputs at the location of La Mortadelle station. Comparison at the other sites yields similar results (Tables S2, S3). The elevation differences between the stations and MAR grid cells are indicated in

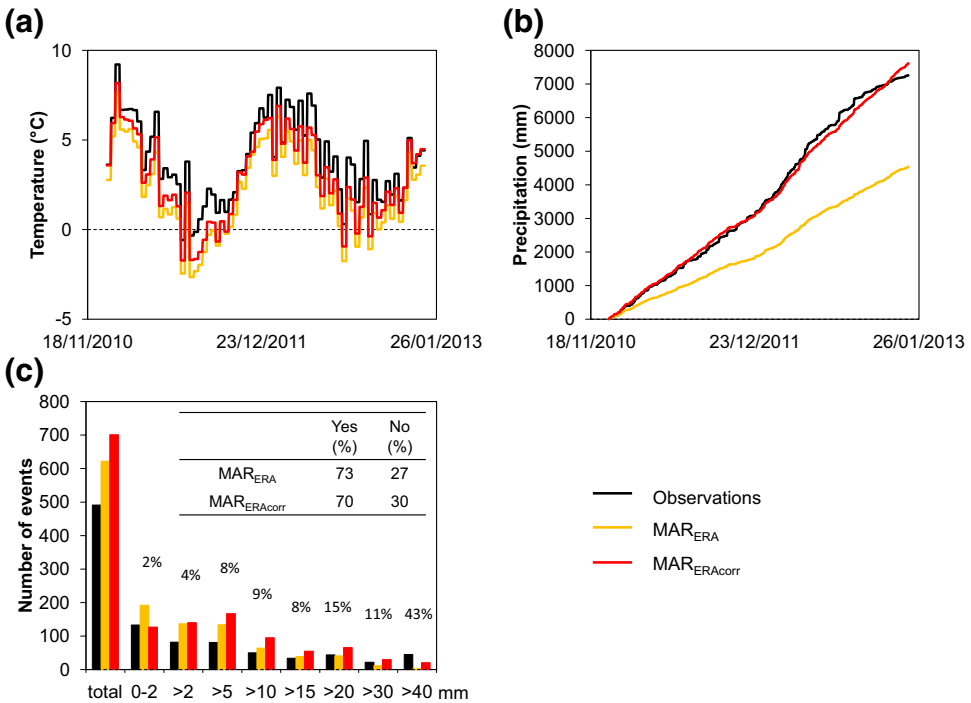

Fig. 2 Comparison between modeled and measured temperature and precipitation at La Mortadelle station in 2011 and 2012 (731 observations): **a** 10-day averaged temperature, **b** accumulated total precipitation, **c** number of daily precipitation events of different intensities (percentages above the charts indicate the ratio of each precipitation class compared to the total observed amounts) and percentages of modeled and observed events in agreement (Yes: both show some precipitation or both show no precipitation) and in disagreement (No: one shows some precipitation while the other shows no precipitation). MAR_{ERA} stands for results of the MAR model forced by ERA-Interim, while $MAR_{ERAcorr}$ represents results of the MAR model forced by ERA-Interim after applying the optimal temperature (+ 0.8 °C) and humidity (+ 10%) corrections at the MAR lateral boundaries

Table 2 Mean observed value and statistics of the comparison between modeled and measured daily temperature and precipitation at La Mortadelle station in 2011 and 2012: Root Mean Square Error (RMSE), correlation between observed and modeled values (R, all values are significant based on a Student's test with $p < 0.05$) and mean annual, summer and winter biases

Variable		Temperature (°C)		Precipitation (mm day^{-1})	
Mean (observation)		3.89		10.0	
Forcing		ERA	ERAcorr	ERA	ERAcorr
RMSE		1.10	1.11	14.9	13.5
R	(-)	0.94	0.94	0.72	0.73
bias	Annual	− 1.70	− 1.02	− 3.7	0.5
	Summer	− 1.65	− 0.90	− 4.5	0
	Winter	− 1.74	− 1.13	− 3.0	1.0

Table S4. This evaluation shows that ERA-Interim is suitable for forcing the MAR model in its present configuration, although modeled precipitation is underestimated in ERA-Interim-driven MAR, which simulates only 75% of observed precipitation or less at every site (Fig. 2b). The model estimates the timing of precipitation events relatively well (model and observations in accordance for more than 70% of cases at La Mortadelle station). However, the intensity of large events (> 20 mm per day), which represent 70% of the total precipitation at La Mortadelle station (and from 21 to 77% at other sites), is usually underestimated by MAR when forced by ERA-Interim (Fig. 2c).

Because of the resolution gap between the driving large-scale model (reanalysis or GCM) and the MAR model, and the fact that the calculation of the saturation humidity in the MAR model could be different from the forcing models, we adjust the humidity field from the forcing model prior to using it to force MAR. To increase the precipitation rate simulated by MAR, we increased humidity in ERA-Interim at each vertical level of the MAR boundaries by different percentages and assessed the improvement of precipitation results in MAR compared to observational data. Different temperature corrections in the forcing fields were also tested (Tables S2, S3). Increasing the humidity in ERA-Interim by 10% greatly improves MAR precipitation results (Fig. 2, Table 2 and Table S3), without affecting significantly temperature (Table S2). In particular, it reduces annual precipitation biases and increases the intensity of large events, thereby improving total precipitation amounts. Temperature biases at the MAR lateral boundaries can also be corrected following Fettweis et al. (2017). Adding 0.8 °C to ERA-Interim (Fig. 2a, Table 2), slightly improves MAR temperature results compared to all stations, except at Sourcils Noirs (Fig. 2, TableS 2, S2). This correction is a good compromise between obtaining reasonable temperature biases at all stations, and not changing too drastically the mean temperature at the boundaries of the MAR, which we expect to have a large impact on the final SMB. Applying such corrections at the MAR lateral boundaries improves the comparison with observations because they compensate some biases of MAR; it does not mean that the ERA-Interim data are wrong.

Near-surface mean temperature and annual accumulated precipitation modeled over 1980–2005 on the Kerguelen Islands by the MAR driven by corrected ERA-Interim fields (Fig. 3) are generally in good agreement with data measured at stations across the archipelago, as already presented above (Fig. 2, Tables S2, S3). In addition, the spatial distribution of temperature and precipitation is in agreement with Fonseca and Martín-Torres (2018). It represents well the foehn effect occurring in this area (Verfaillie 2014) with very wet conditions in the western part of the islands, and drier conditions in the East; this is a recurring feature in Southern mid-latitudes (Neale and Fitzharris 1997; Garreaud et al. 2009). Temperature is mainly correlated with elevation (see Fig. 1 in Berthier et al. (2009) for the topography of the Kerguelen Islands), although at the same elevation temperature is greater downstream of the ice cap than upstream. About 80% less precipitation is measured at Port-aux-Français than at La Mortadelle station [Table S3 and Verfaillie (2014)], which can be partly explained by the elevation difference. This is well captured by the MAR model, which gives high precipitation amounts on the western part of the archipelago—about 3–4 m per year, and up to 7 m per year on the ice cap, similar to what is observed in Patagonia (Garreaud et al. 2013; Schaefer et al. 2013) or in New Zealand (Neale and Fitzharris 1997; Hooker and Fitzharris 1999)—and rather dry conditions on the eastern part (less than 1 m per year on the Courbet Peninsula where Port-aux-Français is located). Those precipitation amounts are also fairly consistent with precipitation simulated by the WRF model in Fonseca and Martín-Torres (2018).

3.2 Evaluation of the MAR surface scheme

3.2.1 Evaluation of the surface mass balance of the MAR

We now focus on MAR results in terms of SMB. Table 3 presents mean SMB values for 1980-2005 on the Cook

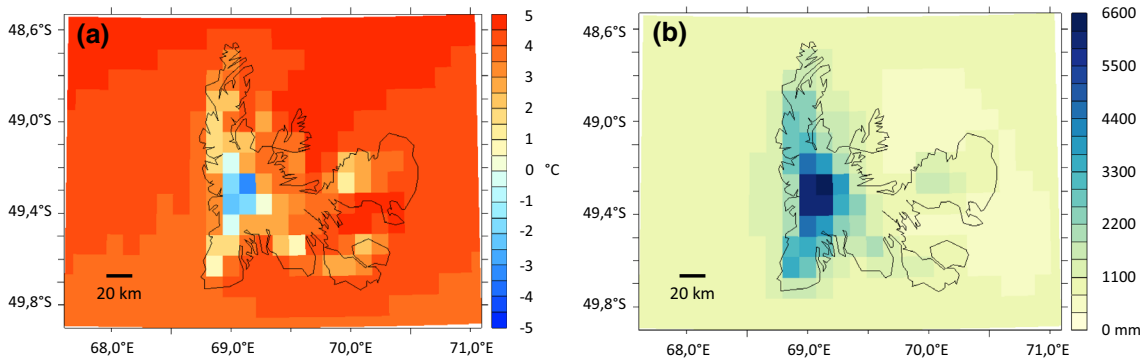

Fig. 3 Maps of 10 km-resolution **a** mean near-surface temperature and **b** accumulated precipitation over 1980-2005 on the Kerguelen Islands simulated by the MAR model forced by ERA-Interim after corrections (humidity increased by 10% and temperature increased by 0.8 °C) at the MAR lateral boundaries

Ice Cap modeled with the MAR forced by ERA-Interim. Because no direct SMB measurement is available from 1980 to 2005, geodetic SMB values obtained from the difference between two digital elevation models, between 1963 and 2000 and between 2000 and 2010 from Favier et al. (2016), are shown for reference. We use the modeling method from Favier et al. (2016), i.e. a positive degree day (PDD) model forced by atmospheric data from the station of Port-aux-Français and MAR-derived temperature and precipitation altitudinal dependency. This yields a modeled SMB of -1.22 ± 0.33 m w.e. a^{-1} for the period 1980-2005 with surfaces and elevations from 2009 (Table 3). Similarly, in this study, the hypsometry of the Cook Ice Cap in 2009 (Verfaillie et al. 2015) was used for calculating the 1980–2005 SMB derived from MAR results at the scale of the whole ice cap, which yields slightly less negative values than if it was integrated on the surfaces and elevations from 2005.

When the MAR is forced by ERA-Interim without correction, the SMB value is the same order of magnitude as SMB measurements and PDD model estimates. Using the corrected (humidity increased by 10% and temperature increased by 0.8 °C) ERA-Interim fields to drive the MAR yields slightly more negative SMB values (difference of -0.27 m w.e. a^{-1}, see Table 3), but still within the uncertainty ranges. The variability of SMB with elevation is well represented in the MAR forced by ERA-Interim fields compared to stake measurements carried out in the 1970s (Fig. 4). However, the MAR is unable to represent the current slope of observed SMB, which is closer to horizontal ("stakes 2011" in Fig. 4).

Table 3 Mean SMB and ice loss for the whole ice cap over the period 1980-2005 from the MAR model forced by ERA-Interim (ERA) and selected CMIP5 models. corr indicates corrected forcings (humidity increased by 10% and 5% respectively for ERA-Interim and ACCESS1-3, and temperature increased by 0.8 °C and decreased by 0.9 °C respectively for ERA-Interim and ACCESS1-3). Measured SMB (m w.e. a^{-1}) from 1963 to 2000 and from 2000 to 2010 (Favier et al. 2016) is also shown for reference, as well as SMB calculated from 1980 to 2005 using the PDD modeling method from Favier et al. (2016)

	Period	Method	SMB (m w.e. a^{-1})	Ice loss (Gt a^{-1})
MAR_{ERA}	1980–2005	MAR model	− 1.32	− 0.51
$MAR_{ERAcorr}$	1980–2005	MAR model	− 1.59	− 0.61
$MAR_{ACCESS1\text{-}3}$	1980–2005	MAR model	− 2.89	− 1.11
$MAR_{ACCESS1\text{-}3corr}$	1980–2005	MAR model	− 1.16	− 0.44
	2006–2100	MAR model	− 4.60	− 1.77
	2090–2100	MAR model	− 7.86	− 3.03
$MAR_{NorESM1\text{-}M}$	1980–2005	MAR model	− 3.47	− 1.33
$MAR_{GISS\text{-}E2\text{-}R}$	1980–2005	MAR model	− 3.63	− 1.40
$MAR_{GFDL\text{-}CM3}$	1980–2005	MAR model	− 4.69	− 1.80
$MAR_{MRI\text{-}CGCM3}$	1980–2005	MAR model	− 9.54	− 3.67
Favier et al. (2016)	1963–2000	Geodetic	-1.33 ± 0.90	− 0.51
Favier et al. (2016)	2000–2010	Geodetic	-1.59 ± 0.19	− 0.61
Favier et al. (2016)	1980–2005	PDD model	-1.22 ± 0.33	− 0.47

3.2.2 Evaluation of the surface energy balance of the MAR

The SMB computed by the MAR model forced by (corrected) ERA-Interim fields is in good agreement with field data, showing a similar gradient with elevation and a similar ELA value as found in Figure 4 of Verfaillie et al. (2015). This is due to a correct modeling of SEB, although the very high quality of SMB partially hides several error compensations. Comparison with measurements done at the Mortadelle's AWS (for which radiation measurements are available) reveals a slight overestimation of the incoming shortwave radiation (*SWi*, difference of + 34 W m^{-2}) which is compensated by lower incoming longwave radiation (*LWi*, difference of − 32 W m^{-2}) in the MAR model compared to observations, although this could also be due to a local artefact at this AWS. MAR values are however similar to those given by ERA and NCEP reanalyses, and those measured at PAF meteorological station (Verfaillie et al. 2015). The potential biases in radiation partly result from a slight underestimation of the cloud cover for the sub-Antarctic regions in the MAR version used in this study (Fettweis et al. 2017). The energy budget was then evaluated for MAR grid cells where the ice mask exceeds 75%, in order to avoid large biases caused by warming of ice-free surfaces in the same cells. Evaluations were performed with SMB and SEB calculations made by Verfaillie et al. (2015) whenever data was available at a similar elevation as the MAR grid cell (Table 4). This was possible for one grid cell (581 m a.s.l.) near the P4 profile presented in Verfaillie et al. (2015), where MODIS albedo calculations and stake data allowed calculations of the SEB. The SMB at the P4 profile was analyzed using 3 stakes with slightly different surface characteristics (Fig. 4). Two stakes are located in areas where some snow overaccumulation was observed. As a result, they yield SMB values that are not extremely negative. The last stake of the P4 profile is located in a zone with lower observed accumulation, resulting in more negative SMB. The computed SMB from the MAR is more similar to data from the overaccumulation zone, reflecting several error compensations. In Verfaillie et al. (2015), a mean albedo value of 0.63 was computed at this location for 2011 using clear sky MODIS images. In this cell, a higher albedo in the MAR compensates for higher incoming shortwave radiation, leading to very similar net shortwave radiation (*SW*). The computed turbulent heat fluxes ($LE + H$) are also close to data provided by Verfaillie et al. (2015) using the approach of Favier et al. (2011) and more reduced than those measured by Poggi (1977a, b). Because the surface temperature modeled by the MAR is very close to the one from Verfaillie et al. (2015), the net longwave radiation (*LW*) results are 30 W m^{-2} more negative, and the final ablation is more reduced. This compensates for lower accumulation simulated by the MAR than observed in Verfaillie et al. (2015), at least for the stakes located in the overaccumulation region. As a consequence, MAR values are very similar to observations around 540 m asl. However, if one considers the points with lower accumulation, then the MAR tends to yield insufficiently negative SMB values in this grid cell (Table 4). However, it must also be kept in mind that precipitation (especially snow) measurements in case of strong winds are

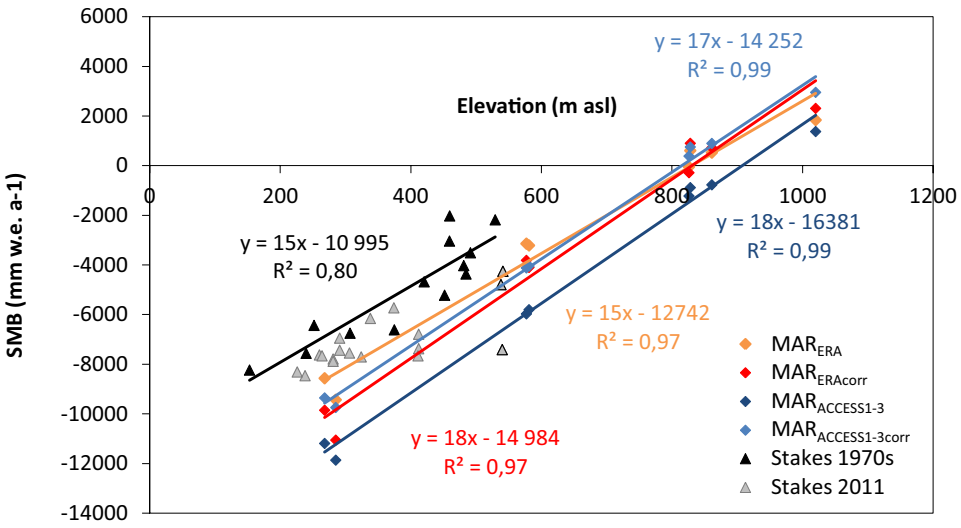

Fig. 4 SMB as a function of elevation on Ampere Glacier: SMB measured with stakes in the 1970s (Vallon 1977a, b, 1987) and in 2011 (Verfaillie et al. 2015), and modeled by the MAR RCM forced by ERA-Interim uncorrected (MAR_{ERA}) and corrected ($MAR_{ERAcorr}$) and ACCESS1-3 uncorrected ($MAR_{ACCESS1\text{-}3}$) and corrected ($MAR_{ACCESS1\text{-}3corr}$) over 1980-2005. Linear regression lines are indicated along with their equations and correlation coefficients. Stakes from the P4 profile in 2011 discussed in Sect. 3.2.2 are represented by grey triangles with black contours

Table 4 Comparison between SEB components estimated from Verfaillie et al. (2015) and from MAR in this study forced by ERA-Interim (ERA) and ACCESS1-3 corrected fields, over 1980–2005, at similar elevations: incoming shortwave radiation (SWi), incoming longwave radiation (LWi), albedo, outgoing longwave radiation (LWo), net shortwave radiation (SW), net longwave radiation (LW), latent heat flux (LE), sensible heat flux (H), LE+H, ablation, snow precipitation (Snow), and surface mass balance (SMB). (1) Using stake SMB values in the observed snow overaccumulation zone of the P4 profile (See Fig. 4), (2) using stake SMB values in the "regular" accumulation zone of the P4 profile, (3) using the MODIS albedo

	Verfaillie et al. (2015)			This study (MAR)			
	MODIS cell	MODIS cell (1)	MODIS cell (2)	ERA corr	ACCESS corr	ERA corr (3)	ACCESS corr (3)
Elevation (m a.s.l.)	540			581	581		
SWi (W m^{-2})	109			143	147		
LWi (W m^{-2})	320			288	283		
Albedo (-)	0.63			0.72	0.71	0.63	0.63
LWo (W m^{-2})	311			309	299		
SW (W m^{-2})	44			41	43	53	54
LW (W m^{-2})	10			−21	−17	−21	−17
LE (W m^{-2})				21	20		
H (W m^{-2})				6	6		
LE+H (W m^{-2})	30			27	26	27	26
Ablation (mm w.e. a^{-1})	−7876	−7876	−7876	−4359	−4962	−5504	−6015
Snow (mm w.e. a^{-1})	870	3351	464	259	919	259	919
SMB (mm w.e. a^{-1})	−7006	−4525	−7412	−4100	−4043	−5245	−5097

often underestimated compared to reality (Larson and Peck 1974; Wagnon et al. 2009). Since precipitation in the MAR is calibrated thanks to precipitation observations, not only do the error compensations within the RCM come into play, but also the precipitation undercatch of rain gauges.

3.3 CMIP5 models selected

The analysis of anomalies presented in Fig. S1 and S2 reveals that the GCM closest to ERA-Interim over 1980-1999 in the Kerguelen region in terms of both temperature and humidity was ACCESS1-3. Its mean anomalies with respect to ERA-Interim are comparable to the mean anomalies of the ERA-40 and NCEP1 reanalyses with respect to ERA-Interim. For the selection of extreme models, the GCMs combining both high temperature biases and low humidity biases should yield the lowest SMB, and the one combining low temperature biases and high humidity biases should provide the highest SMB, once they are used to drive the MAR model. The two most extreme models in terms of temperature were MRI-CGCM3 and GFDL-CM3. GFDL-CM3 presents the coldest biases and MRI-CGCM3 the warmest biases (GISS-E2-H was not considered, as the 6h outputs necessary to force the MAR model were unavailable). However, it is also clear that the models that were most extreme in terms of temperature were not the most extreme in terms of humidity. In fact, GFDL-CM3, which was the coldest, is also too dry compared to ERA-Interim, while MRI-CGCM3, the warmest GCM, is also too humid, which would result in moderate SMB values. This behaviour, common to all CMIP5 models, is somewhat similar to the Clausius-Clapeyron behaviour, which establishes a relation between the amount of precipitable water to the moisture holding capacity of the air, which is itself linked to temperature (e.g., Krinner et al. 2007). To select the two GCMs that would give the most extreme SMB MAR results, it is necessary to compare the joint biases of temperature and humidity of each model with respect to ERA-Interim, as presented in Fig. 5. Biases are calculated, as previously, over 1980–1999 and over the entire 40°-60°S latitudinal belt in order to take into account the potential regional impact of each CMIP5 model on the final MAR SMB results. GISS-E2-R was chosen as the GCM combining both dry and hot biases (the only other dry and hot model, FGOALS-s2, did not have the 6h outputs necessary to force the MAR model), and NorESM1-M as the one combining wet and cold biases (among a selection of GCMs presenting similar biases).

A summary of the temperature and humidity anomalies with respect to ERA-Interim for these five selected CMIP5 GCMs is presented in Figs. 6 and 7. We can see from these figures that the spatial variability of the temperature and humidity anomalies can be high, depending on the model. For example, GFDL-CM3 and NorESM1-M are too cold in almost the entire region of the 40°–60°S latitudinal belt, while other GCMs (ACCESS1-3, GISS-E2-R and MRI-CGCM3) show opposite temperature anomalies to the north

of Kerguelen (with cold anomalies) compared to the south (with warm anomalies). In terms of humidity, the spatial variability in the 40°–60°S latitudinal belt is less pronounced than that of temperature. This demonstrates that mean temperature biases are not sufficient to describe model behavior, and that the choice of model will change according to the region of interest.

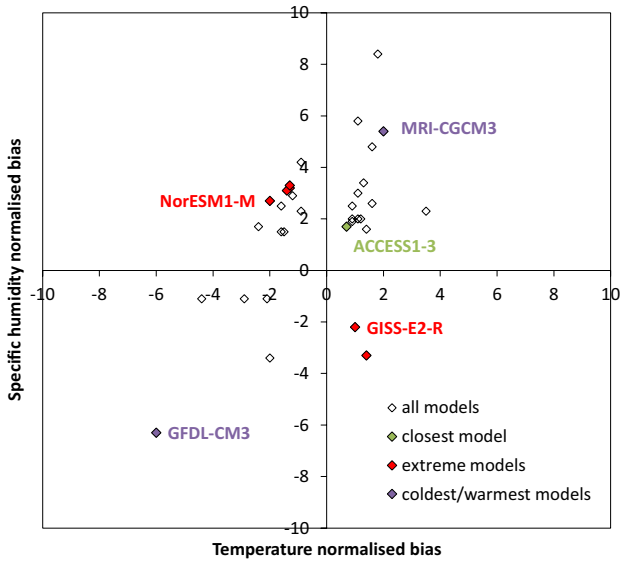

Fig. 5 Plot of the normalized biases of summer temperature (DJF) at 850 hPa for all CMIP5 GCMs with respect to ERA-Interim over 1980–1999 for the entire 40°–60°S latitudinal belt, versus the same normalized biases but for specific humidity at 850 hPa

Additionally, we compared the temporal variability and trends in temperature and precipitation in the five selected models (ACCESS1-3, NorESM1-M, GISS-E2-R, GFDL-CM3 and MRI-CGCM3), and also after downscaling with the MAR model, to observed variability and trends in Table 5. Temperature trends in the CMIP5 models are generally overestimated, although slightly less after downscaling with MAR (differences range between -0.07 °C decade^{-1} and $+0.03$ °C decade^{-1} depending on the model). None of the five selected GCMs are able to reproduce the magnitude of observed decreasing trends in precipitation. NorESM1-M and MRI-CGCM3 display the most negative trends, but they are still around one-tenth of observed trends. Forcing the MAR model by these large-scale models does not systematically improve precipitation trends. Only the precipitation trends from the MAR forced by reanalyses (MAR_{ERA} and $MAR_{ERAcorr}$) are realistic (although still overestimated).

Finally, we calculated the mean spreads in temperature in summer and winter and compared them to observations over 1980–2005. Both the winter and the summer temperature variabilities are underestimated in CMIP5 models compared to observations, especially the summer variability (Table 5).

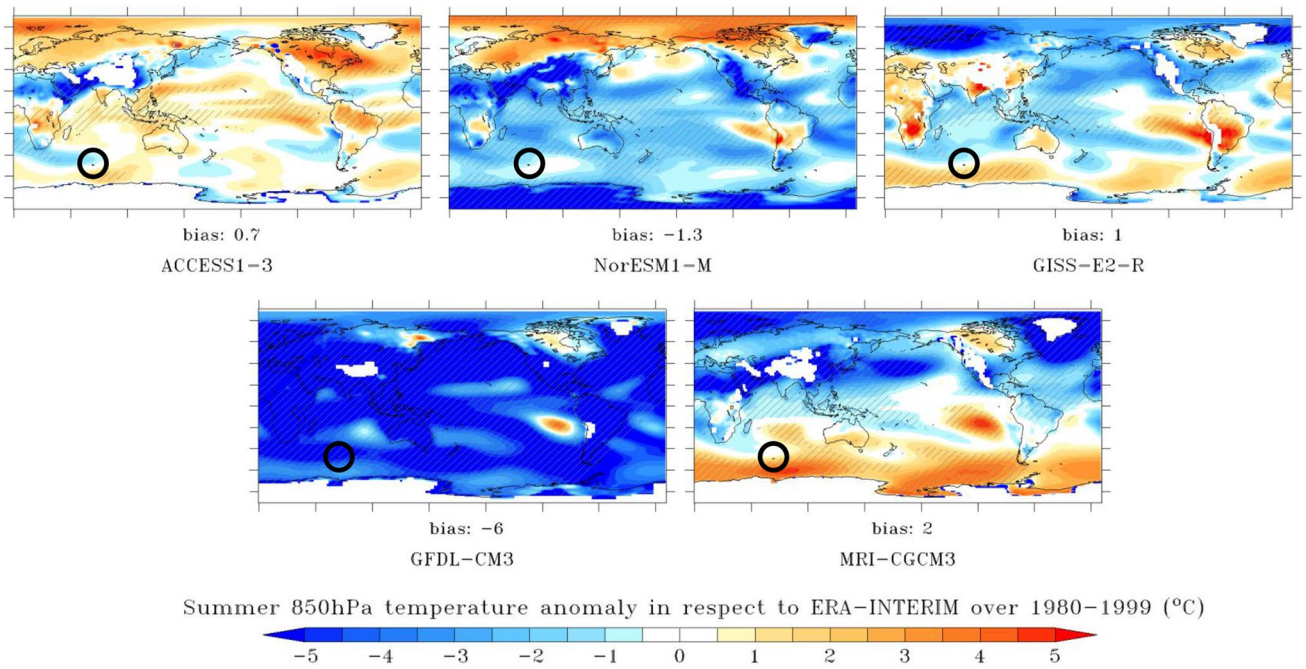

Fig. 6 Mean anomaly ($\overline{T}_{CMIP5} - \overline{T}_{ERA-Int}$) of summer temperature (DJF) at 850hPa with respect to ERA-Interim over 1980–1999, plotted on the ERA-Interim grid, for ACCESS1-3, NorESM1-M, GISS-E2-R, GFDL-CM3 and MRI-CGCM3. Biases indicated are calculated on the whole 40°-60°S latitudinal belt as : ($\overline{T}_{CMIP5} - \overline{T}_{ERA-Int}$)/$\sigma(T_{ERA-Int})$, where σ represents standard deviation. Hatched zones indicate regions where anomalies are more than two times higher than the standard deviation of temperature in ERA-Interim. The black circles indicate the location of the Kerguelen Islands

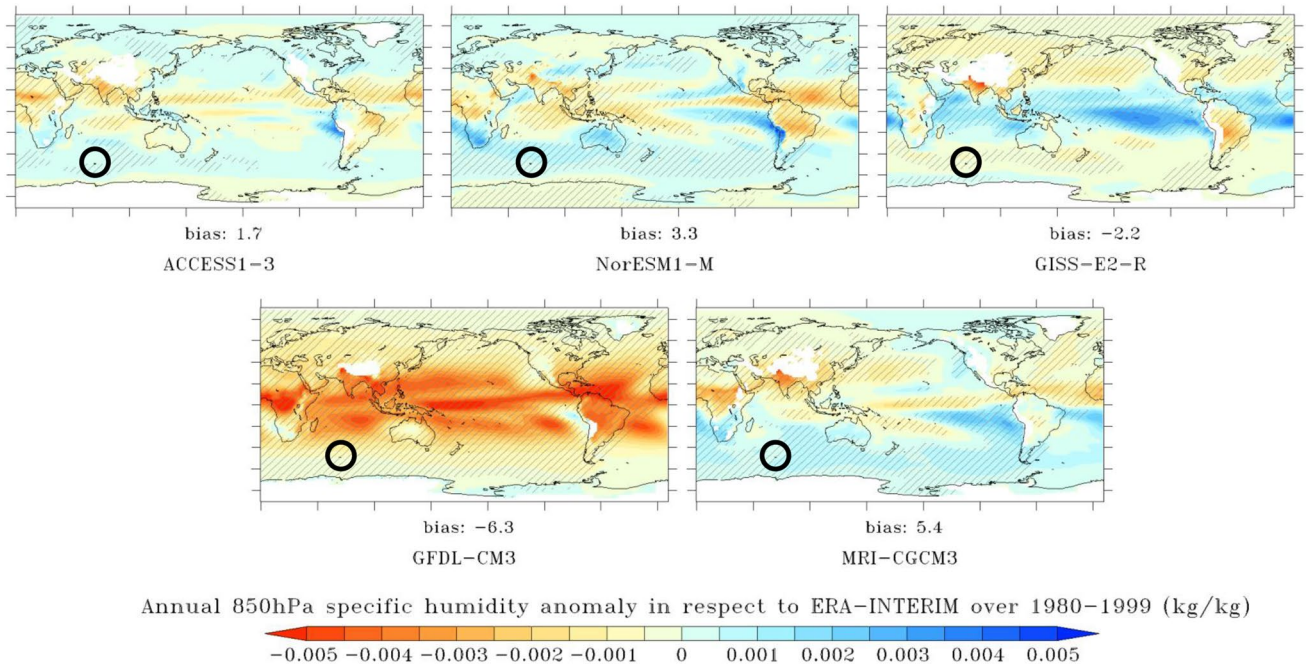

Fig. 7 Same as Fig. 6, but for specific humidity

Both temperature variabilities (summer and winter) are improved when downscaled with the MAR. In the following, we test the impact of these discrepancies on the SMB modeling with the MAR, and assess whether the CMIP5-MAR simulations offer interesting information with regards to the Kerguelen Islands.

3.4 SMB from the MAR forced by selected CMIP5 models

As can be seen in Table 3, mean SMB values from the MAR model over the last decades vary greatly depending on the large-scale model used for forcing. From Table 3, it is clear that SMB values from CMIP5-forced simulations are generally too negative.

3.4.1 Evaluation of the SMB from the MAR forced by ACCESS1-3

The MAR outputs forced by the "reasonable" CMIP5 climate model ACCESS1-3 were compared to long series of data at the scale of the archipelago. These long series correspond to the outputs of MAR forced by corrected ERA-Interim reanalysis fields. We observe that humidity from the ACCESS1-3 simulation needs to be adjusted and increased by 5% to reach acceptable long-term (30 years) precipitation amounts in MAR compared to the simulation forced by ERA-Interim with corrections. Furthermore, we removed 0.9 °C from the ACCESS1-3 forcings to be as close as possible to values from the MAR forced with corrected ERA-Interim fields.

Table 5 Trends of precipitation (P, % change compared to the mean observed value over the period 1980-2005) and temperature (T, °C decade^{-1}) and winter and summer temperature spreads (maximum–minimum, °C) in observations from the Port-aux-Français station and in the five selected CMIP5 GCMs ACCESS1-3, NorESM1-M, GISS-E2-R, GFDL-CM3 and MRI-CGCM3 over 1980-2005. The same calculations for the MAR model forced with those GCMs, and with ERA-Interim (ERA), are also given for comparison

Dataset	P trend (%)	T trend (°C decade^{-1})	Winter T spread (°C)	Summer T spread (°C)
Observation	− 157	− 0.01	10.2	11.6
ACCESS1-3	+ 1	+ 0.09	8.1	4.1
NorESM1-M	− 13	+ 0.10	6.8	5.9
GISS-E2-R	− 5	+ 0.36	5.9	5.0
GFDL-CM3	+ 16	+ 0.34	7.0	3.9
MRI-CGCM3	− 16	+ 0.10	5.8	3.3
MAR_{ERA}	− 190	− 0.09	7.2	6.5
$MAR_{ERAcorr}$	− 310	+ 0.08	7.5	6.2
$MAR_{ACCESS1-3}$	+ 44	+ 0.09	8.5	5.6
$MAR_{ACCESS1-3corr}$	+ 24	+ 0.08	8.8	5.7
$MAR_{NorESM1-M}$	− 56	+ 0.13	9.5	9.7
$MAR_{GISS-E2-R}$	+ 25	+ 0.34	8.1	8.6
$MAR_{GFDL-CM3}$	+ 22	+ 0.33	8.7	4.5
$MAR_{MRI-CGCM3}$	− 16	+ 0.03	10.2	3.9

Correcting ACCESS1-3 fields before driving the MAR allows one to obtain more reasonable SMB values that are closer to ERA-driven values and measurements and SMB pseudo-reference from Favier et al. (2016), even though the values remain very negative (Table 3). Moreover, the evolution of SMB with elevation is very similar to the one obtained with MAR forced by ERA-Interim corrected fields and realistic compared to stake observations from the 1970s, but not from 2011 (Fig. 4).

3.4.2 Analysis of the SMB from extreme CMIP5 models

We analyze the SMB obtained by forcing the MAR model with GCMs initially selected to represent the extremes of SMB on the Cook Ice Cap (Sect. 2.4). Surprisingly, those CMIP5 models fail in reproducing extreme values of SMB (Table 3). NorESM1-M was chosen as the GCM combining both wet and cold biases compared to ERA-Interim, thus meant to yield the less negative MAR SMB. GISS-E2-R, on the other hand, displayed both dry and cold biases, and was thus supposed to yield the most negative MAR SMB. Forcing the MAR with NorESM1-M, however, yields more negative SMB values (Table 3) than ACCESS1-3 (without correction). Moreover, GISS-E2-R displays slightly more negative MAR SMB values than NorESM1-M, but not the most negative ones, as MAR SMB values using GFDL-CM3 or MRI-CGCM3 models are more negative (much more negative in the case of MRI-CGCM3).

3.4.3 Future SMB estimates

For future projections of SMB, we should be able to rely on estimates from MAR driven by corrected ACCESS1-3 fields with some confidence, even though there is no indication that the future trend given by this GCM is correct. Correcting the forcing fields from all CMIP5 models in a similar manner to what was done for ACCESS1-3 would probably require initial humidity and temperature field corrections that are too drastic and unrealistic for most GCMs. Moreover, it would not have provided us with any information on the expected possible spread of values in the future, because it would be suppressed by the adjustment. As a result, only the projections for the (corrected) model considered as the most adequate over the recent period are discussed. MAR driven by corrected ACCESS1-3 fields provides values of SMB of -4.60 m w.e. a^{-1} over the period 2006-2100 and -7.86 m w.e. a^{-1} for the last decade of the twenty-first century (Table 3), assuming present surface extent and elevation. The latter value is difficult to compare to the mean SMB value of -3.22 m w.e. a^{-1} for ACCESS1-3 over the same period from Favier et al. (2016) because the methods for meteorological downscaling and SMB computation are very different. However, both approaches demonstrate that the ice cap will continue to lose mass at a very high rate.

4 Discussion

4.1 Evaluation of MAR atmospherical outputs against observations

The Kerguelen Islands, located in the middle of the ocean and under the influence of a westerly circulation system, represent an ideal setting for regional downscaling analysis and the assessment of CMIP5 models. Temperature and precipitation simulated by the MAR model driven by ERA-Interim were evaluated against 6 stations across the Kerguelen Islands (Sect. 3.1). The comparison showed that MAR driven by ERA-Interim generally reproduced satisfactory temperature and precipitation measurements, but that precipitation was underestimated. This was due to an underestimation of intense precipitation events, as already noted in Verfaillie et al. (2015), which account for 21–77% of total precipitation amounts depending on the station considered. A mean adjustment of temperature and humidity fields in the MAR forcing dataset was necessary to better reproduce station data. These adjustments generally reduced biases in temperature and precipitation simulated by MAR, and increased the proportion of intense precipitation events. Maps of mean annual temperature and cumulated annual precipitation over 1980-2005 from MAR forced by ERA-Interim after those corrections reveal a realistic distribution of these variables across the islands (Fig. 3). The data also show a clear dependence with elevation, which was used to determine the climatic settings over the islands for SMB modeling using a positive degree day model in Favier et al. (2016).

4.2 Evaluation of the MAR surface scheme in terms of SMB and SEB

MAR forced by ERA-Interim correctly reproduces the regional climate settings and the associated SMB and SEB. The good RCM results help to study the spatial distribution of SMB over the Cook Ice Cap. The SMB variation with elevation is largely explained by the increasing amount of snow precipitation with elevation, which results in a quick increase in the albedo and a decrease in the net shortwave radiation budget. The variations of turbulent heat fluxes LE+H are also significantly correlated to elevation, even though the variations of each turbulent heat flux taken independently (H and LE) are poorly linked to this variable alone. The surface temperature is highly correlated with elevation as well, resulting in a progressive decrease in surface energy losses by outgoing longwave radiation (*LWo*). The SEB

from the MAR driven by corrected ERA-Interim fields is satisfactorily close to MODIS-derived estimates from Verfaillie et al. (2015) when similar elevations are compared (about 30% lower in the MAR than in MODIS-derived estimates). However, at the scale of the whole ice cap, some error compensations occur, mainly through an overestimation of the incoming shortwave radiation, compensated by a lower incoming longwave radiation. This is probably due to a slight underestimation (10–20%) of the cloud cover in the MAR version used in this study, which has been largely reduced in the latest version of the MAR (MAR v3.9, see e.g. Wyard et al. 2018).

Other key parameters impacting the spatial distribution of the SEB at the scale of the ice cap are mainly related to the very strong west to east foehn effect over the ice cap. This is visible through the decrease of the cloud cover which results in a quick increase in the *SWi* values (from the west to the east). This increase is largely compensated by the decrease in *LWi* values. This effect extends also westward from the Cook Ice Cap summit. However, since impacts of cloud cover on *LWi* and *SWi* tend to compensate for each other, their impact on the net radiation balance is limited. Turbulent heat flux values are also impacted by the decrease in moisture associated with the foehn effect, nevertheless, the exact consequences are hard to discuss because only few cells present a significant ice cover in our model, and only 5 cells present ice mask values exceeding 75%. In other cells, the warming of tundra surfaces impacts the buoyancy, leading to biased values of turbulent heat fluxes. Yet, changes in turbulent heat fluxes and longwave radiation are largely more reduced than those associated with albedo variations, demonstrating that albedo variations caused by the decreasing snow precipitation amounts are a first order variable explaining the SEB on the Cook Ice Cap (Verfaillie et al. 2015).

However, this key role of albedo in the ablation processes is currently inducing a limitation in our MAR simulations. Our SMB modeling is able to represent the slope of SMB with elevation measured in the 1970s, but not the one measured in 2011. Indeed, in the 1970s, there was still enough snowfall to see a gradual evolution of the snowpack with elevation, i.e. increasing albedo values with elevation. More recently, however, albedo became almost uniform on the ice cap due to the large disappearance of snowpack and firn, leading to the presence of bare ice over large parts of the glacier. As a result, melt rates increased and became more uniform and the slope of observed SMB with elevation became much flatter (Fig. 4). However, since ERA-Interim data is only available since 1979, it was impossible in our model to reproduce the full firn removal that occurred since the beginning of the 1960s. Nearly 20 years of negative SMB were missing in our spin-up period to correctly reproduce the current observed surface state, i.e. with a similarly low albedo between the front and 800 m asl. As a consequence, our SMB modeling is not able to reproduce the current surface state of the ice cap.

4.3 Selection of CMIP5 models and resulting SMB

For large ice caps, it has been demonstrated that important feedbacks between temperature and melting occur, and thus mass balance anomalies in the MAR model due to temperature anomalies will tend to be amplified with time because a GCM which is too warm will produce a rapid melt of the ice cap in MAR and thus mass balance values that are too negative (and vice-versa for a GCM which is too cold). One can thus reasonably assume that the GCM simulating best the temperature (and circulation) conditions over the recent period for these large ice caps will be the most suitable for at least near-future projections, and that current extreme GCMs will continue to diverge in the future (Fettweis et al. 2013). For future SMB estimates, the model selection approach (Fettweis et al. 2013) we used indicated the Australian GCM ACCESS1-3 as the most appropriate for our region of interest. It was also the model chosen as the most pertinent for forcing RCMs over Antarctica in Agosta et al. (2015). This seems logical considering that the physics of the GCM is probably adapted to Southern mid- and high-latitudes (Bi et al. 2013). Additionally, two GCMs were selected in order to represent the extremes of SMB on the ice cap due to their combined temperature and humidity biases (NorESM1-M and GISS-E2-R), and two other GCMs which displayed cold and warm conditions in the subantarctic region (GFDL-CM3 and MRI-CGCM3) were also tested.

We observed that this method fails for the Kerguelen Archipelago. SMB from the MAR model forced by ACCESS1-3 from 1980 to 2005 is too negative. Even the forcing fields from this GCM selected as most appropriate based on mean meteorological fields must be corrected in order to yield SMB results close to geodetic measurements and PDD estimates. The GCMs initially selected as extremes did not provide the ensemble variability we were trying to find as they failed in giving the most extreme values of SMB. This was already observed in Favier et al. (2016), who showed that the CMIP5 multi-model mean and the majority of GCMs were not able to reproduce the Cook Ice Cap wastage from the 1950s onwards, mainly due to an incorrect representation of the decrease in precipitation in the Kerguelen region. Here we confirm this finding, showing that the five GCMs selected in this study present very different trends in temperature and precipitation, and that no model is able to reproduce the observed trend in precipitation. Most GCMs follow a Clausius-Clapeyron law (Krinner et al. 2007; Agosta et al. 2013; Palerme et al. 2017), where humidity increases with increasing temperature. Only two models display dry and warm biases, among which GISS-E2-R, which did not yield the expected most negative SMB after forcing

the MAR. This is also due to the fact that our GCM selection is based on an assessment of the mean biases in temperature and humidity compared to ERA-Interim, but the temporal variability (e.g. the drying trend) is not taken into account because the models do not reflect the observations.

4.4 Reducing means biases in CMIP5 models is still not sufficient

Furthermore, in Favier et al. (2016), a reduction of the mean interannual biases of temperature and precipitation was applied to each CMIP5 GCM in order to better reproduce the local climate settings and SMB. Indeed, because model outputs were largely biased in the Kerguelen region, the temperature bias over the period 1951-2005 was removed from each GCM by subtracting the mean bias, whereas precipitation rates were divided by the mean ratio between observations and the model. This approach allowed us to show that the ensemble mean model (EMM) SMB value was similar to the one computed with the observed climate data from Kerguelen Islands, but assuming an hypothetical situation without drying. Here, we analyzed more deeply ablation in each simulation from Favier et al. (2016), and observed that modeling biases were significantly correlated to summer temperature biases rather than the annual temperature biases. Thus, we reproduced the Favier et al. (2016) approach but removing the summer temperature bias over the period 1951–2005 from each GCM. This approach slightly improves the EMM SMB results (not shown), but the final trend is still close to the one obtained assuming an hypothetical situation without drying because the precipitation trend is not correctly reproduced in CMIP5 models. This means that neither removing the mean annual nor mean summer biases in GCMs is sufficient to compute further SMB values, and a more complex bias correction (of the whole probability distribution) is required.

Here, in addition, we show that the temporal evolution of SMB cannot be explained solely by the corresponding evolution in temperature and precipitation (Fig. 8). For example, MAR forced by MRI-CGCM3 yields the steepest trend in SMB even though the trends in (decreasing) precipitation and (increasing) temperature are not the strongest of all the different models used (see Table 5 for trend values). Although temperature and precipitation are the main drivers of SMB in the Kerguelen region, other drivers exist (e.g., radiation and albedo) that should be taken into account when analyzing the temporal evolution of SMB.

MAR SMB projections indicate that significant shrinking of the Cook Ice Cap is expected to continue through the twenty-first century, as projected in Favier et al. (2016), even though the SMB value for ACCESS1-3 for the end of the century can hardly be compared to the mean value obtained for ACCESS1-3 from the update of the method from Favier et al. (2016) because this study and Favier et al. (2016) use different methods. However, it is not possible to validate the future trends, and the ensemble variability of SMB projections using CMIP5 models cannot be assessed as it still has not been obtained for the recent period using the model selection method from Fettweis et al. (2013). Possible refinements to the selection method could have been performed. Sea-level pressure could have been included in the selection of CMIP5 models, or precipitable water could have been taken into account instead of the 850 hPa specific humidity, similarly to what was done in Agosta et al. (2015). However, as noted above, most models are unable to capture the spatial pattern and temporal variability of observed precipitation trends in the southern Indian Ocean correctly. This will remain a key aspect that prevents us from deriving realistic projections of SMB changes, regardless of the selection method.

5 Conclusions

In our study we show the good quality of the MAR model in reproducing the regional atmospheric settings, SMB and SEB over the Cook Ice Cap. When the MAR is forced by accurate large-scale forcing such as ERA-Interim, it provides accurate SMB time series and realistic variability compared to observations. However, it fails when forced by "biased" GCMs. Moreover, we show that the MAR RCM also fails in simulating accurate SMB time series and realistic variability when it is forced by CMIP5 models selected against observations, even after removing their mean temperature and humidity biases.

Indeed those GCM models represent precious tools to assess global climate change and the link between temperature and greenhouse gases, and to highlight the large-scale changes in the main climatic modes and circulation. However, we show from a relatively simple case study that robust observed changes in climatic modes and circulation are not simulated at the regional scale. This is the case for example of the increase in the Southern Annular Mode and the resulting observed storm track shift. Only the multi-model mean temperature is consistent with reality. As a result, CMIP5 models are useful, when considering their mean value, where general circulation patterns are not so important (i.e., temperature is the first order variable). But they need to be considered with caution in regions where important circulation changes occurred and will likely continue to occur in the future (Favier et al. 2016).

A possible solution would be to improve bias-adjustment methods in these regions. To this end, sophisticated adjustment methods such as quantile-mapping (Déqué 2007; Gobiet et al. 2015; Verfaillie et al. 2017) are appealing. However, they need robust, long-term and spatially dense

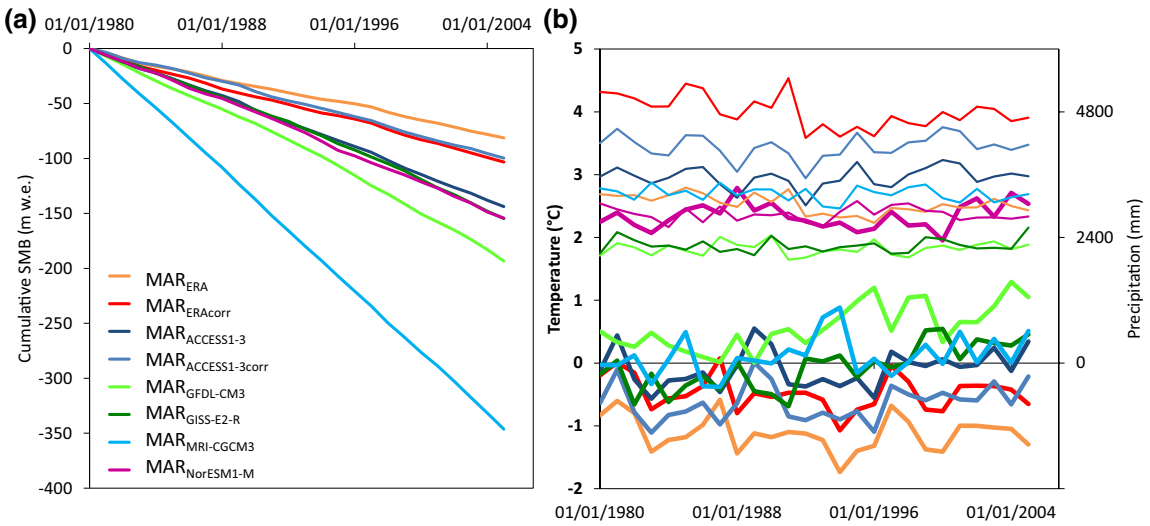

Fig. 8 Temporal evolution of **a** cumulative SMB and **b** temperature (bold lines) and precipitation (regular lines) between 1980 and 2005 in the MAR model forced by ERA-Interim (ERA) and selected CMIP5 models. corr indicates corrected forcings (humidity increased by 10% and 5% respectively for ERA-Interim and ACCESS1-3, and temperature increased by 0.8 °C and decreased by 0.9 °C respectively for ERA-Interim and ACCESS1-3)

measurement series (or fine-scale reanalyses) to operate, which are available in Northern regions such as the Alps, but rare in the Southern mid-latitudes. Combining bias-adjustment with spectral nudging, as proposed by Guldberg et al. (2005) and Kharin and Scinocca (2012), would be another seductive solution. Finally, further improvements of decadal-scale modeling in these regions where circulation changes occur seem to remain a prerequisite to any realistic projections of the future evolution of glaciers and ice caps.

Acknowledgements This study was funded by IPEV-1048 GLACIOCLIM-KESAACO and LEFE-INSU KCRuMBLE programs. Deborah Verfaillie's work has been partially funded by the European project EUCP (H2020-SC5-2016-776613). Logistical supply to the Kerguelen Islands was provided by the French Polar Institute (IPEV). We particularly thank Météo France for the meteorological data from PAF. ERA-Interim reanalysis data were downloaded from the ECMWF data portal at http://apps.ecmwf.int/archive-catalogue/. We acknowledge the World Climate Research Program's Working Group on Coupled Modelling, which is responsible for CMIP, and we thank the climate modeling groups (listed in Supplementary Table 1) for producing and making available their model outputs. Regional climate modeling was performed using the Froggy platform of the CIMENT infrastructure (https://ciment.ujf-grenoble.fr), which is supported by the Rhône-Alpes region (GRANT CPER07_13 CIRA), the OSUG@2020 labex (reference ANR10 LABX56) and the Equip@Meso project (reference ANR-10-EQPX-29-01) of the programme Investissements d'Avenir supervised by the Agence Nationale pour la Recherche. We would like to thank Rachel H. White and Marcus Falls for their help with language editing, and the Editor and an anonymous Reviewer for their constructive comments during the review of this article.

Compliance with ethical standards

Conflicts of interest The authors declare that they have no conflict of interest.

References

Agosta C, Favier V, Krinner G, Gallée H, Fettweis X, Genthon C (2013) High resolution modelling of the Antarctic surface mass balance, application for the twentieth, twenty first and twenty second centuries. Clim Dyn 41(11–12):3247–3260

Agosta C, Fettweis X, Datta R (2015) Evaluation of the CMIP5 models in the aim of regional modelling of the Antarctic surface mass balance. Cryosphere 9:2311–2321. https://doi.org/10.5194/tc-9-2311-2015

Amante C, Eakins B (2009) ETOPO1 1 arc-minute global relief model: procedures, data sources and analysis. NOAA technical memorandum NESDIS NGDC-24

Bechtold P, Bazile E, Guichard F, Mascart P, Richard E (2001) A mass-flux convection scheme for regional and global models. Q J R Meteorol Soc 127(573):869–886

Berthier E, Le Bris R, Mabileau L, Testut L, Remy F (2009) Ice wastage on the Kerguelen Islands (49 degrees S, 69 degrees E) between 1963 and 2006. J Geophys Res 114:F03005. https://doi.org/10.1029/2008JF001192

Bi D, Dix M, Marsland S, OFarrell S, Rashid H, Uotila P, Hirst A, Kowalczyk E, Golebiewski M, Sullivan A, Yan H, Hannah N, Franklin C, Sun Z, Vohralik P, Watterson I, Zhou X, Fiedler R, Collier M, Ma Y, Noonan J, Stevens L, Uhe P, Zhu H, Griffies S, Hill R, Harris C, Puri K (2013) The ACCESS coupled model: description, control climate and evaluation. Austral Meteorol Oceanogr J 63(1):41–64

Brun E, David P, Sudul M, Brunot G (1992) A numerical model to simulate snowcover stratigraphy for operational avalanche forecasting. J Glaciol 38(1):13–22

Cabré MF, Solman S, Núñez M (2016) Regional climate change scenarios over southern South America for future climate (2080–2099) using the MM5 model: mean, interannual variability and uncertainties. Atmósfera 29(1):35–60

De Ridder K, Gallée H (1998) Land surface-induced regional climate change in southern Israel. J Appl Meteorol 37(11):1470–1485

Dee D, Uppala S, Simmons A, Berrisford P, Poli P, Kobayashi S, Andrae U, Balmaseda M, Balsamo G, Bauer P, Bechtold P, Beljaars A, van de Berg L, Bidlot J, Bormann N, Cand Delsol R, Dragani Fuentes M, Geer A, Haimberger L, Healy S, Hersbach H, Hólm E, Isaksen L, Kållberg P, Köhler M, Matricardi M, McNally A, Monge-Sanz B, Morcrette JJ, Park BK, Peubey C, de Rosnay P, Tavolato C, Thépaut JN, Vitart F (2011) The ERA-interim reanalysis: configuration and performance of the data assimilation system. Q J R Meteorol Soc 137:553–597. https://doi.org/10.1002/qj.828

Delworth T, Zeng F (2014) Regional rainfall decline in Australia attributed to anthropogenic greenhouse gases and ozone levels. Nat Geosci 7:583–587. https://doi.org/10.1038/ngeo2201

Déqué M (2007) Frequency of precipitation and temperature extremes over France in an anthropogenic scenario: model results and statistical correction according to observed values. Glob Planet Change 57(1):16–26. https://doi.org/10.1016/j.gloplacha.2006.11.030

Duynkerke P, van den Broeke M (1994) Surface energy balance and katabatic flow over glacier and tundra during GIMEX-91. Glob Planet Change 9(1):17–28

Falvey M, Garreaud R (2009) Regional cooling in a warming world: recent temperature trends in the southeast Pacific and along the west coast of subtropical South America (1979–2006). J Geophys Res 114:D04102. https://doi.org/10.1029/2008JD010519

Favier V, Agosta C, Genthon C, Arnaud L, Trouvillez A, Gallée H (2011) Modeling the mass and surface heat budgets in a coastal blue ice area of Adelie Land, Antarctica. J Geophys Res Earth Surf 116:F03017. https://doi.org/10.1029/2010JF001939

Favier V, Verfaillie D, Berthier E, Menegoz M, Jomelli V, Kay J, Ducret L, Malbéteau Y, Brunstein D, Gallée H, Park Y, Rinterknecht V (2016) Atmospheric drying as the main driver of dramatic glacier wastage in the southern Indian Ocean. Sci Rep 6:32396. https://doi.org/10.1038/srep32396

Fettweis X, Franco B, Tedesco M, van Angelen J, Lenaerts J, van den Broeke M, Gallée H (2013) Estimating Greenland ice sheet surface mass balance contribution to future sea level rise using the regional atmospheric climate model MAR. Cryosphere 7(2):469–489

Fettweis X, Box JE, Agosta C, Amory C, Kittel C, Lang C, van As D, Machguth H, Gallée H (2017) Reconstructions of the 1900–2015 Greenland ice sheet surface mass balance using the regional climate MAR model. Cryosphere 11(2):1015

Fitzharris B, Chinn T, Lamont G (1997) Glacier balance fluctuations an atmospheric circulation patterns over the Southern Alps, New Zealand. Int J Clim 17:745–763. https://doi.org/10.1002/(SICI)1097-0088(19970615)

Fitzharris B, Clare G, Renwick J (2007) Teleconnections between Andean and New Zealand glaciers. Glob Planet Change 59(1–4):159–174. https://doi.org/10.1016/j.gloplacha.2006.11.022

Fonseca R, Martín-Torres J (2018) High-resolution dynamical downscaling of re-analysis data over the Kerguelen Islands using the WRF model. Theor Appl Climatol. https://doi.org/10.1007/s00704-018-2438-0

Fouquart Y, Bonnel B (1980) Computations of solar heating of the earth's atmosphere—a new parameterization. Beiträge zur Physik der Atmosphäre 53:35–62

Frenot Y, Gloaguen JC, Picot G, Bougre J, Benjamin D (1993) Azorella selago Hook. Used to estimate glacier fluctuations and climatic history in the Kerguelen Islands over the last two centuries. Oecologia 95:140–144. https://doi.org/10.1007/BF00649517

Frenot Y, Gloaguen JC, Van de Vijver B, Beyens L (1997) Datation of some Holocene peat sediments and glacier fluctuations in the Kerguelen Islands. Comptes Rendus de l'Académie des Sciences, Série III-Sci de la Vie - Life Sci 320(7):567–573. https://doi.org/10.1016/S0764-4469(97)84712-9

Gallée H, Duynkerke P (1997) Air-snow interactions and the surface energy and mass balance over the melting zone of west Greenland during the Greenland ice margin experiment. J Geophys Res 102(D12):13813–13824. https://doi.org/10.1029/96JD03358

Gallée H, Schayes G (1994) Development of a three-dimensional meso-γ primitive equation model: Katabatic winds simulation in the area of Terra Nova Bay, Antarctica. Mon Weather Rev 122(4):671–685

Gallée H, Guyomarc'h G, Brun E (2001) Impact of snow drift on the Antarctic ice sheet surface mass balance: possible sensitivity to snow-surface properties. Bound Layer Meteorol 99(1):1–19. https://doi.org/10.1023/A:1018776422809

Garreaud R, Vuille M, Compagnucci R, Marengo J (2009) Present-day South American climate. Palaeogeogr Palaeoclimatol Palaeoecol 281:180–195. https://doi.org/10.1016/j.palaeo.2007.10.032

Garreaud R, Lopez P, Minvielle M, Rojas M (2013) Large-scale control on the Patagonian climate. J Clim 26(1):215–230

Gobiet A, Suklitsch M, Heinrich G (2015) The effect of empirical-statistical correction of intensity-dependent model errors on the temperature climate change signal. Hydrol Earth Syst Sci 19(10):4055–4066. https://doi.org/10.5194/hess-19-4055-2015

Guldberg A, Kaas E, Déqué M, Yang S, Thorsen S (2005) Reduction of systematic errors by empirical model correction: impact on seasonal prediction skill. Tellus A 57(4):575–588. https://doi.org/10.1111/j.1600-0870.2005.00120.x

Hooker B, Fitzharris B (1999) The correlation between climatic parameters and the retreat and advance of Franz Josef Glacier, New Zealand. Glob Planet Change 22(1):39–48. https://doi.org/10.1016/S0921-8181(99)00023-5

Jomelli V, Mokadem F, Schimmelpfennig I, Chapron E, Rinterknecht V, Favier V, Verfaillie D, Brunstein D, Legentil C, Michel E, Swingedouw D, Jaouen A, Aumaitre G, Bourlès DL, Keddadouche K (2017) Sub-Antarctic glacier extensions in the Kerguelen region (49° S, Indian Ocean) over the past 24,000 years constrained by ^{36}Cl moraine dating. Quat Sci Rev 162:128–144

Jomelli V, Schimmelpfennig I, Favier V, Mokadem F, Landais A, Rinterknecht V, Brunstein D, Verfaillie D, Legentil C, Aumaitre G, Bourlès DL, Keddadouche K (2018) Glacier extent in sub-Antarctic Kerguelen Archipelago from MIS 3 period: evidence from ^{36}Cl dating. Quat Sci Rev 183:110–123

Kalnay E, Kanamitsu M, Kistler R, Collins W, Deaven D, Gandin L, Iredell M, Saha S, White G, Woollen J, Zhu Y, Leetmaa A, Reynolds R, Chelliah M, Ebisuzaki W, Higgins W, Janowiak J, Mo K, Ropelewski C, Wang J, Roy J, Dennis J (1996) The NCEP/NCAR 40-Year reanalysis project. Bull Am Meteorol Soc 77(3):437–471

Kessler E (1969) On the distribution and continuity of water substance in atmospheric circulation, vol 10. American Meteorological Society, Boston

Kharin V, Scinocca J (2012) The impact of model fidelity on seasonal predictive skill. Geophys Res Lett 39:L18803. https://doi.org/10.1029/2012GL052815

Krinner G, Magand O, Simmonds I, Genthon C, Dufresne JL (2007) Simulated Antarctic precipitation and surface mass balance at the end of the twentieth and twenty-first centuries. Clim Dyn 28(2–3):215–230. https://doi.org/10.1007/s00382-006-0177-x

Larson L, Peck E (1974) Accuracy of precipitation measurements for hydrologic modeling. Water Resour Res 10(4):857–863. https://doi.org/10.1029/WR010i004p00857

Lefebre F, Gallée H, Van Ypersele JP, Greuell W (2002) Modelling of snow and ice melt at ETH-Camp (West Greenland): a study of surface albedo. J Geophys Res. https://doi.org/10.1029/2001JD001160

Lin YL, Farley R, Orville H (1983) Bulk parameterization of the snow field in a cloud model. J Clim Appl Meteorol 22(6):1065–1092

Marzeion B, Jarosch A, Hofer M (2012) Past and future sea-level change from the surface mass balance of glaciers. Cryosphere 6(6):1295–1322. https://doi.org/10.5194/tc-6-1295-2012

Ménégoz M, Gallée H, Jacobi H (2013) Precipitation and snow cover in the Himalaya: from reanalysis to regional climate simulations. Hydrol Earth Syst Sci 17(10):3921–3936. https://doi.org/10.5194/hess-17-3921-2013

Monin A, Obukhov A (1954) Basic laws of turbulent mixing in the surface layer of the atmosphere. Contrib Geophys Inst Acad Sci USSR 24(151):163–187

Morcrette JJ (2002) Assessment of the ECMWF model cloudiness and surface radiation fields at the ARMSGP site. Mon Weather Rev 130(2):257–277

Neale S, Fitzharris B (1997) Energy balance and synoptic climatology of a melting snowpack in the Southern Alps, New Zealand. Int J Climatol 17(14):1595–1609

Palerme C, Genthon C, Claud C, Kay J, Wood N, L'Ecuyer T (2017) Evaluation of current and projected Antarctic precipitation in CMIP5 models. Clim Dyn 48(1–2):225–239. https://doi.org/10.1007/s00382-016-3071-1

Poggi A (1977a) Etude comparative du bilan thermique en deux stations du glacier Ampère Iles Kerguelen. Zeitschrift für Gletscherkunde und Glazialgeologie 13:87–97

Poggi A (1977b) Heat Balance in ablation area of Ampere Glacier (Kerguelen Islands). J Appl Meteorol 16:48–55

Purich A, Cowan T, Min SK, Cai W (2013) Autumn precipitation trends over Southern Hemisphere midlatitudes as simulated by CMIP5 models. J Clim 26(21):8341–8356. https://doi.org/10.1175/JCLI-D-13-00007.1

Radić V, Bliss A, Beedlow AC, Hock R, Miles E, Cogley JG (2014) Regional and global projections of twenty-first century glacier mass changes in response to climate scenarios from global climate models. Clim Dyn 42(1–2):37–58. https://doi.org/10.1007/s00382-013-1719-7

Schaefer M, Machguth H, Falvey M, Casassa G (2013) Modeling past and future surface mass balance of the Northern Patagonia Icefield. J Geophys Res Earth Surf 118(2):571–588. https://doi.org/10.1002/jgrf.20038

Solomon S, Qin D, Manning M, Chen Z, Marquis M, Averyt K, Tignor M, Miller H (2007) IPCC, 2007: Climate change 2007: The physical science basis. Contribution of Working Group I to the fourth assessment report of the Intergovernmental Panel on Climate Change

Takeuchi Y, Naruse R, Satow K, Ishikawa N (1999) Comparison of heat balance characteristics at five glaciers in the southern hemisphere. Glob Planet Change 22(1):201–208. https://doi.org/10.1016/S0921-8181(99)00037-5

Taylor K, Stouffer R, Meehl G (2012) An overview of CMIP5 and the experiment design. Bull Am Meteorol Soc 93(4):485–498

Thompson D, Solomon S, Kushner P, England M, Grise K, Karoly D (2011) Signatures of the Antarctic ozone hole in Southern Hemisphere surface climate change. Nat Geosci 4:741–749. https://doi.org/10.1038/ngeo1296

Uppala S, Kållberg P, Simmons A, Andrae U, Bechtold V, Fiorino M, Gibson J, Haseler J, Hernandez A, Kelly G, Li X, Onogi K, Saarinen S, Sokka N, Allan R, Andersson E, Arpe K, Balmaseda M, Beljaars A, Van De Berg L, Bidlot J, Bormann N, Caires S, Chevallier F, Dethof A, Dragosavac M, Fisher M, Fuentes M, Hagemann S, Hólm E, Hoskins B, Isaksen L, Janssen P, Jenne R, Mcnally A, Mahfouf JF, Morcrette JJ, Rayner N, Saunders R, Simon P, Sterl A, Trenberth K, Untch A, Vasiljevic D, Viterbo P, Woollen J (2005) The ERA-40 re-analysis. Q J R Meteorol Soc 131(612):2961–3012. https://doi.org/10.1256/qj.04.176

Vallon M (1977a) Bilan de masse et fluctuations récentes du Glacier Ampère (Iles Kerguelen, TAAF). Zeitschrift für Gletscherkunde und Glazialgeologie 13:55–85

Vallon M (1977b) Topographie sous glaciaire du Glacier Ampère (Iles Kerguelen, TAAF). Zeitschrift für Gletscherkunde und Glazialgeologie 13:37–55

Vallon M (1987) Glaciologie à Kerguelen. In: Actes du Colloque sur la Recherche Française dans les Terres Australes, Strasbourg

Verfaillie D (2014) Suivi et modélisation du bilan de masse de la calotte Cook aux Îles Kerguelen - lien avec le changement climatique. PhD thesis, Université Joseph Fourier, Grenoble

Verfaillie D, Favier V, Dumont M, Jomelli V, Gilbert A, Brunstein D, Gallée H, Rinterknecht V, Menegoz M, Frenot Y (2015) Recent glacier decline in the Kerguelen Islands (49° S, 69° E) derived from modeling, field observations and satellite data. J Geophys Res 120(3):637–654. https://doi.org/10.1002/2014JF003329

Verfaillie D, Déqué M, Morin S, Lafaysse M (2017) The method ADAMONT v1.0 for statistical adjustment of climate projections applicable to energy balance land surface models. Geosci Model Dev 10:4257–4283. https://doi.org/10.5194/gmd-10-4257-2017

Wagnon P, Lafaysse M, Lejeune Y, Maisinsho L, Rojas M, Chazarin J (2009) Understanding and modelling the physical processes that govern the melting of the snow cover in a tropical mountain environment in Ecuador. J Geophys Res 114:D19113. https://doi.org/10.1029/2009JD012292

Wang G, Kay W (2013) Climate-change impact on the 20th-century relationship between the Southern Annular Mode and global mean temperature. Sci Rep 3:2039. https://doi.org/10.1038/srep02039

Wyard C, Doutreloup S, Belleflamme A, Wild M, Fettweis X (2018) Global radiative flux and cloudiness variability for the Period 1959–2010 in Belgium: a comparison between reanalyses and the regional climate model MAR. Atmosphere 9(7):262. https://doi.org/10.3390/atmos9070262

Yen YC (1981) Review of thermal properties of snow, ice and sea ice. Tech. rep, CRREL Hanover